

# Sub-0.5 nm Equivalent Oxide Thickness Scaling for Si-Doped $Zr_{1-x}Hf_xO_2$ Thin Film without Using Noble Metal Electrode

Ji-Hoon Ahn<sup>\*,†</sup> and Se-Hun Kwon<sup>\*,‡,§</sup>

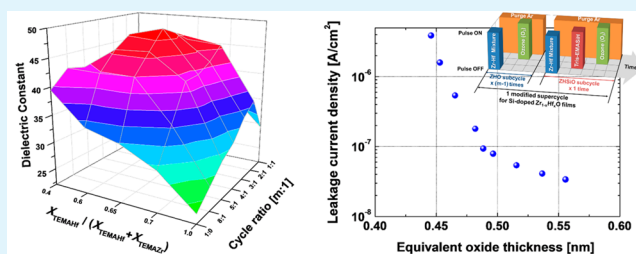
<sup>†</sup>Center for Artificial Low Dimensional Electronic Systems, Institute for Basic Science (IBS), 77 Cheongam-Ro, Pohang 790-784, Republic of Korea

<sup>‡</sup>Global Frontier Center for Hybrid Interface Materials, <sup>§</sup>School of Materials Science and Engineering, Pusan National University, 30 Jangjeon-Dong Geumjeong-Gu, Busan 609-735, Republic of Korea

## Supporting Information

**ABSTRACT:** The dielectric properties of the Si-doped  $Zr_{1-x}Hf_xO_2$  thin films were investigated over a broad compositional range with the goal of improving their properties for use as DRAM capacitor materials. The Si-doped  $Zr_{1-x}Hf_xO_2$  thin films were deposited on TiN bottom electrodes by atomic layer deposition using a TEMA-Zr/TEMA-Hf mixture precursor for deposition of  $Zr_{1-x}Hf_xO_2$  film and Tris-EMASiH as a Si precursor. The Si stabilizer increased the tetragonality and the dielectric constant; however, at high fractions of Si, the crystal structure degraded to amorphous and the dielectric constant decreased. Doping with Si exhibited a larger influence on the dielectric constant at higher Hf content. A Si-doped Hf-rich  $Zr_{1-x}Hf_xO_2$  thin film, with tetragonal structure, exhibited a dielectric constant of about 50. This is the highest value among all reported results for Zr and Hf oxide systems, and equivalent oxide thickness (EOT) value of under 0.5 nm could be obtained with a leakage current of under  $10^{-7}$  A·cm<sup>-2</sup>, which is the lowest EOT value ever reported for a DRAM storage capacitor system without using a noble-metal-based electrode.

**KEYWORDS:** dielectrics, MIM capacitor, thin film, doped-oxide, atomic layer deposition



## INTRODUCTION

As the size of the dynamic random access memory (DRAM) is scaled down, the new high- $k$  dielectric materials, such as  $TiO_2$ <sup>1–3</sup> and  $SrTiO_3$ ,<sup>4–6</sup> have received considerable attention. However, these high- $k$  materials require electrodes based on noble metals (such as Ru and Ir), because they have a relatively narrow band gap, and for acceptable dielectric characteristics, it is necessary to control the crystallinity at the interface between the dielectric and bottom electrode material, is needed. Noble metal electrodes for DRAM applications have been studied for over a decade; however, their mass production has been met with challenges including the difficulty of their conformal deposition in 3-D structures with high aspect ratio, the high cost of the noble metal, and the compatibility of their deposition with other processing steps. Moreover, in the applicable thickness range for DRAM capacitors (around 7 nm), acceptable values of the dielectric constant are not straightforward to obtain because the dielectric properties of high- $k$  materials generally depend on their thickness, which is related to their crystallinity. Oxides of Zr and Hf are currently used in the mass production of complementary metal oxide semiconductor (CMOS) industry, and, especially,  $ZrO_2$  film deposited by atomic layer deposition is used as a dielectric with combining with ultrathin  $Al_2O_3$  layer in current DRAM capacitor. Improving their dielectric properties is as important as developing new high- $k$  materials with regards to enhancing

the technical capabilities and process compatibility of electronic devices. The dielectric properties of Zr-, Hf-based oxides have been extensively studied in view of experiment<sup>7–9</sup> and theory.<sup>10–12</sup> The known crystal structures of  $ZrO_2$  or  $HfO_2$  are monoclinic, cubic, or tetragonal depending on preparation temperature, and tetragonal  $ZrO_2$  and  $HfO_2$  have the highest dielectric constant compared with the other crystal structures of these oxides. Especially, the calculated dielectric constant by the first principle of tetragonal  $HfO_2$  is about 70,<sup>12</sup> which has not been obtained experimentally until now, whereas that of tetragonal  $ZrO_2$  is about 40. Unfortunately, it is difficult to obtain the tetragonal phase under the conditions of DRAM processing, because the tetragonal structure is stable at high temperature. The thermodynamically stable phase at ambient conditions is monoclinic, and has a much lower dielectric constant than the tetragonal phase. Much research has been focused on obtaining a high dielectric constant by stabilizing the tetragonal structure  $ZrO_2$  or  $HfO_2$  by doping, e.g., Si doping of  $HfO_2$ , Er doping of  $HfO_2$ , and Y doping of  $ZrO_2$ ,<sup>13–15</sup> and Park et al. reported remarkable enhancement of dielectric constant ( $\sim 47$ ) by Al doping in relatively thick  $HfO_2$  film.<sup>16</sup> Although, there are some previous reports on

Received: May 18, 2015

Accepted: June 30, 2015

Published: June 30, 2015

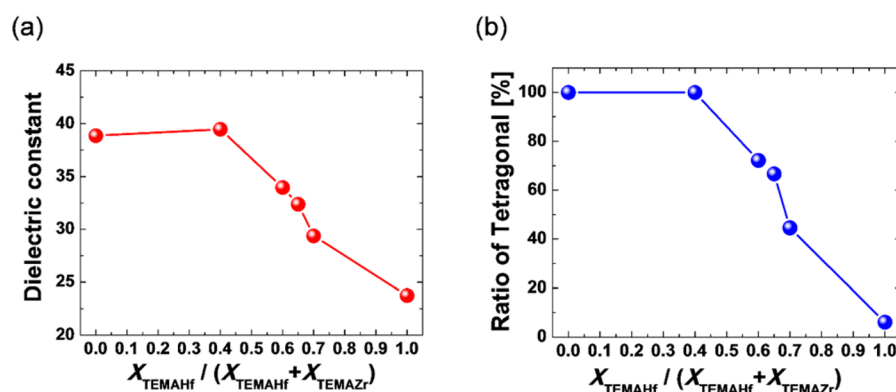


**Figure 1.** Influence of Hf content in the mixture precursor on the (a) dielectric constant, (b) tetragonal ratio of the deposited films that is defined as the intensity of the tetragonal peak as a percentage of the (tetragonal-peak intensity + monoclinic-peak intensity).

undoped<sup>17–19</sup> or nanocrystal embedded Zr–Hf-mixed oxides<sup>20–22</sup> for gate dielectric, the research about combinations of Zr and Hf oxides in ternary metal oxide systems, which include matrices of ZrHf-mixed oxide and stabilizer dopant, for DRAM capacitor have rarely been reported.

In this paper, we investigate the dielectric properties and crystal structure of Si-doped  $\text{Zr}_{1-x}\text{Hf}_x\text{O}_2$  thin films having a broad compositional range, with the goal of maximizing their dielectric properties to extend their performance in DRAM capacitors. The properties of the binary Zr–Hf oxide are first investigated, and then we report about the extension of compositional window for tetragonal structure by Si doping and the outstanding enhancement of EOT scaling by improving dielectric properties without requiring a noble metal electrode.

## EXPERIMENTAL SECTION

Thin films of Si-doped  $\text{Zr}_{1-x}\text{Hf}_x\text{O}_2$  were deposited on TiN (20 nm)/ $\text{SiO}_2/p$ -type Si using atomic layer deposition (ALD). The mixture precursors of tetrakis(ethylmethylamino)zirconium [TEMAZr] and tetrakis(ethylmethylamino)hafnium [TEMAHf], combined in molar ratios of 60:40, 40:60, 35:65, 30:70, and 0:100, were used for deposition of  $\text{Zr}_{1-x}\text{Hf}_x\text{O}_2$  films and Tris(ethylmethylamino)silane [Tris-EMASiH] was used as a precursor for Si doping. The ratio of Zr to Hf in the films was controlled by the molar ratio of precursors. In this work, the coefficients  $a$  and  $b$  in  $\text{Zr}_a\text{Hf}_b$  denote the molar ratio of TEMAZr to TEMAHf =  $a:b$  in the precursor mixture. The process temperature was kept at 280 °C, and ozone, at a concentration of 280  $\text{g}^{-3}$ , was used as an oxidant. For uniform doping of a small amount of Si into  $\text{Zr}_{1-x}\text{Hf}_x\text{O}_2$  films, the films were deposited by a modified supercycle composed of  $(m - 1)$  subcycles of ZrHfO and one subcycle of ZrHfSiO (see Figure S1 in the Supporting Information). The ZrHfSiO subcycle for Si doping was composed of six steps: (1) feeding of the ZrHf precursor mixture, (2) purging, (3) feeding of the Si precursor, (4) purging, (5) feeding of ozone, and (6) purging; otherwise, the normal subcycle of ALD was composed of 4 steps: (1) feeding of the source, (2) purging, (3) feeding of the reactant, and (4) purging. This method is favorable for uniformly incorporating small amounts of dopant, because the Si precursor only adsorbs on residual sites not already occupied by the precursor mixture on the bare surface then. In this paper, ZrHfO-to-SiO ratio =  $m:1$  denotes the case of  $(m - 1)$  subcycles of ZrHfO and one subcycle of ZrHfSiO for Si doping.

To evaluate their dielectric properties and physical properties, 7 nm thick Si-doped  $\text{Zr}_{1-x}\text{Hf}_x\text{O}_2$  films were deposited on TiN substrates that had been formed by chemical vapor deposition using  $\text{TiCl}_4$  and  $\text{NH}_3$  at 650 °C. Prior to film deposition, TiN surface was treated by ozone preflow for 120 s for to minimize the unwanted reaction during initial stage of film deposition, and the as-deposited films underwent rapid thermal annealing at 600 °C for 2 min under  $\text{N}_2$  ambient for the crystallization. The crystal structure of the Si-doped  $\text{Zr}_{1-x}\text{Hf}_x\text{O}_2$  thin

films was determined by X-ray diffraction (XRD, X-pert APD, Philips) in  $2\theta$  scan mode using  $\text{Cu K}\alpha$  radiation ( $\lambda = 1.5405 \text{ \AA}$ ). The composition of the films was determined by X-ray photoelectron spectroscopy (XPS, PHI-Quantum 2000) using a  $\text{Mg K}\alpha$  X-ray source. The electrical properties were measured by fabricating metal–insulator–metal (MIM) capacitors, with a top electrode of TiN deposited by plasma-enhanced ALD using tetrakis(dimethylamido)-titanium [TDMAT] and  $\text{N}_2$  plasma at 270 °C. The area of the planar pattern, which was defined by photolithography, was approximately 20 000  $\mu\text{m}^2$ . The dielectric constant was measured using a  $C$ – $V$  analyzer (Keithley 590) at a frequency of 10 kHz.

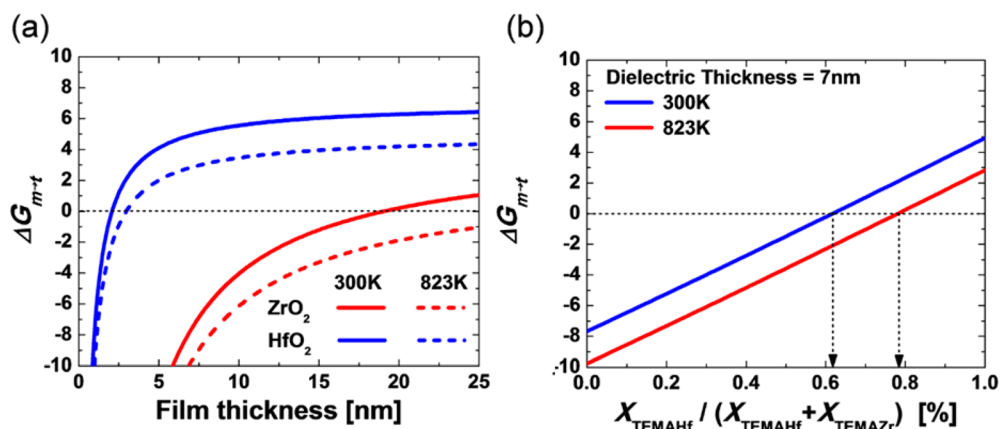
## RESULTS AND DISCUSSION

Figure 1a,b shows the how the dielectric constant and crystallinity of  $\text{Zr}_{1-x}\text{Hf}_x\text{O}_2$  thin films varies with Hf content in the ZrHf mixture precursor, prior to Si doping test. The composition ratio of Zr to Hf in the deposited film had an almost linear relationship with the molar ratio of precursors (see Figure S2 in the Supporting Information). The dielectric constant was not remarkably changed in Zr-rich region, and then decreased with increasing Hf content, in perfect correspondence to the variation of the tetragonal ratio, which is defined as the intensity of the tetragonal peak as a percentage of the (tetragonal-peak intensity + monoclinic-peak intensity). When the  $\text{Zr}_{100}\text{Hf}_0$  or  $\text{Zr}_{60}\text{Hf}_{40}$  mixture precursor was used, the resulting  $\text{Zr}_{1-x}\text{Hf}_x\text{O}_2$  film exhibited only the tetragonal structure; the tetragonal ratio decreased with increasing Hf content in the  $\text{Zr}_{1-x}\text{Hf}_x\text{O}_2$  film. Finally, in the case of the  $\text{Zr}_0\text{Hf}_{100}$  precursor mixture (which in fact contains only the Hf precursor), the film crystallinity was almost monoclinic in structure.

The relationship between the crystal structure and composition of  $\text{Zr}_{1-x}\text{Hf}_x\text{O}_2$  films is explained by a simple thermodynamic model. For a negative difference in Gibbs free energy between the monoclinic and tetragonal structure,  $\Delta G_{m \rightarrow t}$  a transformation of structure can occur at an arbitrary temperature  $T$ . The change of Gibbs free energy corresponding to the transformation can be written as follows

$$\Delta G_{m \rightarrow t} = \Delta H_{m \rightarrow t} - T\Delta S_{m \rightarrow t} + A\Delta\gamma_{m \rightarrow t}$$

where  $\Delta H_{m \rightarrow t}$  is the difference in bulk enthalpy between the monoclinic and tetragonal structures,  $\Delta S_{m \rightarrow t}$  is the difference in bulk entropy between the monoclinic and tetragonal structure, and  $\Delta\gamma_{m \rightarrow t}$  is the surface energy contribution. The specific surface is defined as  $A = V_m/t$ , where  $V_m$  is the molar volume, and  $t$  is the film thickness. The Gibbs free energy difference between the two crystal structures for  $\text{ZrO}_2$  and  $\text{HfO}_2$  by



**Figure 2.** Variation in the difference in Gibbs free energy between the monoclinic and tetragonal structure (a) with films thickness for  $\text{ZrO}_2$  and  $\text{HfO}_2$ , and (b) with Hf content in  $\text{Zr}_{1-x}\text{Hf}_x\text{O}_2$  thin films at a film thickness of 7 nm.

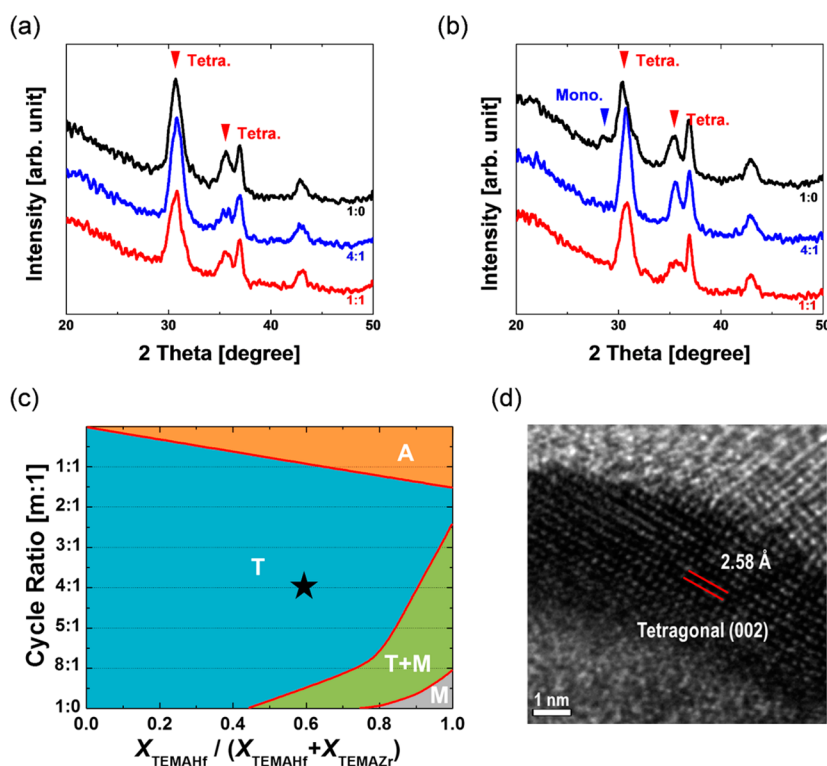


**Figure 3.** Variation of XRD patterns by Si doping in (a)  $\text{Zr}_{0.6}\text{Hf}_{0.4}\text{O}_2$  and (b)  $\text{Zr}_{0.4}\text{Hf}_{0.6}\text{O}_2$  thin films. (c) Schematic of crystallinity of the Si-doped  $\text{Zr}_{1-x}\text{Hf}_x\text{O}_2$  thin films as the ZrHf cycles:Si cycle [m:1], with the Hf contents in ZrHf mixture precursor. (d) Cross-sectional TEM image of Si-doped  $\text{Zr}_{0.4}\text{Hf}_{0.6}\text{O}_2$  at marked sample in panel c.

adding a surface energy term was calculated using the literature values<sup>23</sup> given in Table S1 in the Supporting Information. Figure 2a shows that in the case of  $\text{ZrO}_2$ , the transformation to tetragonal structure occurs when the film thickness becomes less than 19 nm, due to contribution of surface energy reduction as structure transformation is more important than bulk energy term. In the case of  $\text{HfO}_2$ , however, the film thickness must be less than 2 nm to form the tetragonal structure. Furthermore, as shown in Figure 2b of the variation of Gibbs free energy with mol % of Hf in the  $\text{Zr}_{1-x}\text{Hf}_x\text{O}_2$  thin films, assuming that the film thickness is 7 nm and the simple mixing rule applies, thermodynamically stable tetragonal- $\text{Zr}_{1-x}\text{Hf}_x\text{O}_2$  films are formed when the Hf mol % was less than 61% at room temperature and less than 79% at an annealing temperature of 600 °C. Although a few hypotheses

are included, the results of the thermodynamic calculations are in agreement with experimental results demonstrating that it difficult to obtain the tetragonal structure, whose dielectric constant is relatively high, at higher Hf content. Therefore, there is a limit to increasing the dielectric constant above 40 in  $\text{Zr}_{1-x}\text{Hf}_x\text{O}_2$  systems without enhancement of their tetragonality by doping with a stabilizer. Because of these results, the change of crystallinity and the enhancement of dielectric properties of  $\text{Zr}_{1-x}\text{Hf}_x\text{O}_2$  thin films by small amounts of Si doping were investigated.

We investigated the variation of crystallinity of Si-doped  $\text{Zr}_{1-x}\text{Hf}_x\text{O}_2$  thin films in various composition range by XRD analysis and representative XRD peaks of Zr-rich  $\text{Zr}_{1-x}\text{Hf}_x\text{O}_2$  films and Hf-rich  $\text{Zr}_{1-x}\text{Hf}_x\text{O}_2$  films is shown in Figure 3a,b, respectively. Whereas the crystal structure of Zr-rich

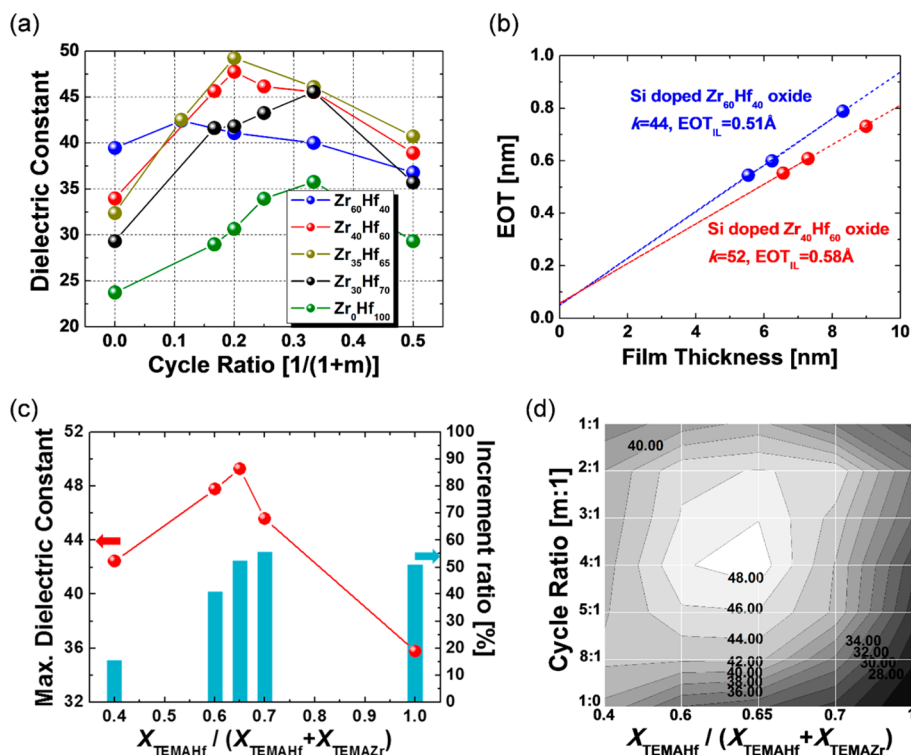


**Figure 4.** (a) Dependence of the dielectric constant of the Si-doped  $Zr_{1-x}Hf_xO_2$  thin films on cycle ratio, [Si cycle/(Si cycle + ZrHf cycles)], on the molar ratio of Zr and Hf in the precursor mixture, and (b) dependence of the EOT values on the thickness of the Si-doped  $Zr_{1-x}Hf_xO_2$  thin films deposited from  $Zr_{60}Hf_{40}$  precursor and  $Zr_{40}Hf_{60}$  precursor. (c) Influence of Hf content on the maximum dielectric constant (line + symbol) and increment ratio of dielectric constant (bar) of the Si-doped  $Zr_{1-x}Hf_xO_2$  thin films. (d) Contour map showing the variation in dielectric constant of the Si-doped  $Zr_{1-x}Hf_xO_2$  thin films as the ZrHf cycles:Si cycle [ $m:1$ ] with the Hf content in the precursor mixtures.

$Zr_{1-x}Hf_xO_2$  film was not remarkably changed by Si doping, the crystal structure of Hf-rich  $Zr_{1-x}Hf_xO_2$  film was changed from mixed phase of monoclinic and tetragonal to only tetragonal phase. Figure 3c shows a schematic mapping of crystallinity versus cycle ratio. The general trend was that the crystallinity was changed from monoclinic to tetragonal by doping of Si into  $Zr_{1-x}Hf_xO_2$  thin films; however, excess doping caused the structure to degrade to amorphous phase. Lee et al.,<sup>10</sup> using density functional theory, calculated the stability of the tetragonal structure of  $HfO_2$  containing cation dopants. The ionic radius of the Si dopant (0.26 Å) is significantly smaller than those of Hf or Zr atoms (0.83–0.84 Å). Therefore, Si dopant tends to shorten the dopant–oxygen bonds. In the tetragonal structure, four Hf–O bonds are already shorter than the others, thereby facilitating the formation of stable dopant–oxygen bonds with relatively small lattice distortions. In addition, an increase in the minimum required amount of Si dopant to achieve the tetragonal phase transformation was observed with increasing Hf content in the Si-doped  $Zr_{1-x}Hf_xO_2$  thin films. This may be attributed to the increase in Gibbs free energy, which is necessary for the phase transformation, with increasing Hf content. For single metal oxide systems, the Gibbs free energy for the monoclinic-to-tetragonal transformation is always larger for the Hf-based system than for the Zr-based system.<sup>24</sup> Therefore, it is apparent that the Zr-rich  $Zr_{1-x}Hf_xO_2$  film transforms more easily to a tetragonal structure with a smaller amount of Si doping. The cross-sectional transmission electron microscopy image of sample of Si-doped  $Zr_{1-x}Hf_xO_2$  thin films with composition of marked point in Figure 3c shows uniformly well crystallized films (see Figure 3d) and the measured interplanar distances

was about 0.258 nm, which is consistent with the (002) plane of the tetragonal phase (0.262 and 0.263 nm for (002) of tetragonal  $HfO_2$  and  $ZrO_2$ ).

Figure 4a shows how the dielectric constant of the Si-doped  $Zr_{1-x}Hf_xO_2$  thin films varies according to the molar ratio of Zr versus Hf in the mixture precursor, and the cycle ratio, which controls the level of Si doping (the cycle ratio is defined as SiO cycle/[SiO cycle + ZrHfO cycles], and is equal to  $=1/[1+m]$  for ZrHfO-to-SiO ratio =  $m:1$ ). Regardless of the molar ratio of the components in the mixture precursor, the dielectric constant increased and then decreased with increasing the amount of Si doping. This is because the crystal structure initially changed from monoclinic to tetragonal when smaller amounts of Si were doped into the films, but degraded to amorphous phase upon excess doping (see Figure 3c). And increasing the Hf content in the mixture precursor increased the Si cycle ratio at which the maximum dielectric constant was obtained, because a greater amount of Si doping was required for the transformation to the tetragonal phase. Figure 4b shows the linear fitting of equivalent oxide thickness (EOT) values as a function of thickness of the Si-doped  $Zr_{1-x}Hf_xO_2$  thin films having a Zr-to-Hf molar ratio of 40:60 and 60:40 in the mixture precursor. Although using the  $Zr_{60}Hf_{40}$  precursor yielded a Si-doped  $Zr_{1-x}Hf_xO_2$  film with a dielectric constant of about 44, except the interfacial layer effect, using the  $Zr_{40}Hf_{60}$  precursor yielded a film with a dielectric constant of about 52 when the Si cycle ratio was 0.2, which corresponds to Si content of about 3 at. %. This is the highest value among all reported results for the Zr-, Hf-based oxide system or TiN bottom electrode systems. In addition, both films exhibited relatively low EOT values of interfacial layer ( $EOT_{IL}$ ), obtained from the y-axis

intercept, which might attribute to ozone pretreatment prior to film deposition. Figure 4c shows the maximum dielectric constant of the Si-doped  $Zr_{1-x}Hf_xO_2$  thin films, as a function of the Hf content in the ZrHf mixture precursor and the increment ratio of the dielectric constant, which is defined by [(maximum dielectric constant–minimum dielectric constant)/minimum dielectric constant] at an arbitrary Zr/Hf ratio in the mixture precursor. With increasing Hf content, doping with Si had a larger effect on the dielectric constant and the largest dielectric constant was obtained at Hf content of  $\sim 65\%$  in the precursor mixture, because with increasing Hf content, the window to form the tetragonal structure becomes narrower and it becomes difficult to obtain only tetragonal phase without amorphous or monoclinic phases and the dielectric constant, calculated by first-principles, becomes larger with increasing Hf content. In other words, the decrease of dielectric constant with Hf content of about 65% as the central figure is due to the lower dielectric constant of tetragonal  $ZrO_2$  than that of tetragonal  $HfO_2$  for Zr-rich Si-doped  $Zr_{1-x}Hf_xO_2$  films and due to the degradation of crystallinity to amorphous phase for Hf contents of above  $\sim 70\%$ . Figure 4d shows a contour map of the dielectric constant of Si-doped  $Zr_{1-x}Hf_xO_2$  thin films over a wide range of compositions. The shape of the dielectric constant contour is very similar to that of the variation in crystallinity, as shown in Figure 3c. This indicates that the dielectric constant of the Si-doped  $Zr_{1-x}Hf_xO_2$  thin films is very closely related to the change in crystal structure.

Finally, we investigated the EOT scalability of Si-doped  $Zr_{1-x}Hf_xO_2$  thin films for a MIM capacitor as shown in Figure 5. Because the tetragonal structure improves the dielectric

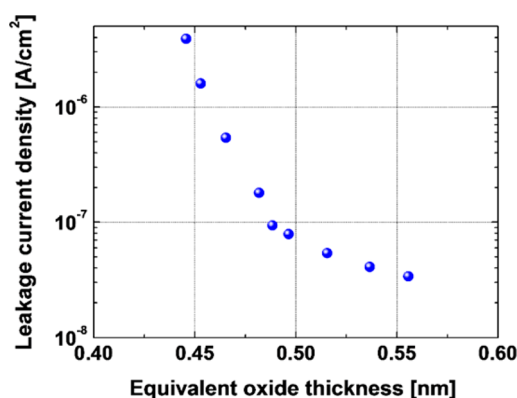


**Figure 5.** Leakage current density at 0.8 V as a function of the EOT values for the Si-doped  $Zr_{1-x}Hf_xO_2$  thin films.

properties, the lowest EOT value, under 0.5 nm with low leakage current density ( $<10^{-7}$  A·cm<sup>-2</sup>) was obtained without using a noble-metal-based electrode. This is the best data for MIM capacitor without a noble metal; the lowest value of EOT ever reported was about 6.1 Å.<sup>25</sup> The data are furthermore comparable with the best results for new higher-k dielectrics, such as  $TiO_2$  and  $SrTiO_3$ , assembled onto noble metal electrodes.<sup>2,3</sup> Thus, the Si-doped  $Zr_{1-x}Hf_xO_2$  thin film proposed by this work is a highly promising candidate for DRAM MIM capacitor applications.

## CONCLUSION

The dielectric properties and crystal structure of Si-doped  $Zr_{1-x}Hf_xO_2$  thin films, and their relationship to the Zr-to-Hf ratio in the mixture precursor and the amount of Si doping,

were investigated to evaluate how adjustments in film composition can extend the performance of Zr and Hf oxides as DRAM capacitor dielectrics. Increasing the amount of Si doping caused the crystal structure to change from monoclinic to tetragonal to the amorphous phase. The dielectric constant increased with the monoclinic-to-tetragonal transformation, and then decreased when the structure became amorphous and the dielectric constant exhibited a larger variation with Si doping as the Hf content increased. Consequently, a Si-doped Hf-rich  $Zr_{1-x}Hf_xO_2$  thin film, with tetragonal structure, exhibited a dielectric constant of about 50. This is the highest value among all reported results for the Zr-, Hf-based oxide system, and the lowest EOT value ever reported for a DRAM MIM capacitor material without using a noble-metal-based electrode.

## ASSOCIATED CONTENT

### Supporting Information

Schematic of the modified ALD supercycle, influence of Hf content in the mixture precursor on the atomic percent of Hf in deposited film, bulk parameters used for thermodynamic calculation, and comparison of the dielectric properties of this study with previous reports for the Zr- or Hf-based oxide system. The Supporting Information is available free of charge on the ACS Publications website at DOI: 10.1021/acsami.5b04303.

## AUTHOR INFORMATION

### Corresponding Authors

\*J.-H. Ahn. E-mail: ajh1820@ibs.re.kr.

\*S.-H. Kwon. E-mail: sehun@pusan.ac.kr.

### Notes

The authors declare no competing financial interest.

## ACKNOWLEDGMENTS

This work was supported by the Global Frontier R&D Program (2013-073298) on Center for Hybrid Interface Materials (HIM) funded by the Ministry of Science, ICT & Future Planning.

## REFERENCES

- (1) Kim, S. K.; Choi, G. J.; Lee, S. Y.; Seo, M.; Lee, S. W.; Han, J. H.; Ahn, H. S.; Han, S.; Hwang, C. S. Al-Doped  $TiO_2$  Films with Ultralow Leakage Currents for Next Generation DRAM Capacitors. *Adv. Mater.* **2008**, *20*, 1429–1435.
- (2) Kim, S. K.; Lee, S. W.; Han, J. H.; Lee, B.; Han, S.; Hwang, C. S. Capacitors with an Equivalent Oxide Thickness of  $< 0.5$  nm for Nanoscale Electronic Semiconductor Memory. *Adv. Funct. Mater.* **2010**, *20*, 2989–3003.
- (3) Jeon, W.; Yoo, S.; Kim, H. K.; Lee, W.; An, C. H.; Chung, M. J.; Cho, C. J.; Kim, S. J.; Hwang, C. S. Evaluating the Top Electrode Material for Achieving an Equivalent Oxide Thickness Smaller than 0.4 nm from an Al-Doped  $TiO_2$  Film. *ACS Appl. Mater. Interfaces* **2014**, *6*, 21632–21637.
- (4) Lee, W.; Han, J. H.; Jeon, W.; Yoo, Y. W.; Lee, S. W.; Kim, S. K.; Ko, C. H.; Lansalot-Matras, C.; Hwang, C. S. Atomic Layer Deposition of  $SrTiO_3$  Films with Cyclopentadienyl-Based Precursors for Metal-Insulator-Metal Capacitors. *Chem. Mater.* **2013**, *25*, 953–961.
- (5) Kim, J. Y.; Ahn, J. H.; Kang, S. W.; Kim, J. H.; Roh, J. S. Effect of Crystallinity and Nonstoichiometric Region on Dielectric Properties of  $SrTiO_3$  Films Formed on Ru. *Appl. Phys. Lett.* **2007**, *91*, 092910.
- (6) Longo, V.; Leick, N.; Roozeboom, F.; Kessels, W. M. M. Plasma-Assisted Atomic Layer Deposition of  $SrTiO_3$ : Stoichiometry and

Crystallinity Studied by Spectroscopic Ellipsometry. *ECS J. Solid State Sci. Technol.* **2013**, *2* (1), N15–N22.

(7) Müller, J.; Böske, T. S.; Schröder, U.; Reiniche, M.; Oberbeck, L.; Zhou, D.; Weinreich, W.; Kücher, P.; Lemberger, M.; Frey, L. Improved Manufacturability of ZrO<sub>2</sub> MIM Capacitors by Process Stabilizing HfO<sub>2</sub> Addition. *Microelectron. Eng.* **2009**, *86*, 1818–1821.

(8) Spiga, S.; Rao, R.; Lamagns, L.; Wiemer, C.; Congede, G.; Lamperti, A.; Molle, A.; Fanciulli, M.; Palma, F.; Irrera, F. Structural and Electrical Properties of Atomic Layer Deposited Al-doped ZrO<sub>2</sub> Films and of the Interface with TaN Electrode. *J. Appl. Phys.* **2012**, *112*, 014107.

(9) Toomey, B.; Cherkaoui, K.; Monaghan, S.; Djara, V.; O'Connor, E.; O'Connell, D.; Oberbeck, L.; Tois, E.; Blomberg, T.; Newcomb, S. B.; Hurley, P. K. The Structural and Electrical Characterization of a HfErO<sub>x</sub> Dielectric for MIM Capacitor DRAM Applications. *Microelectron. Eng.* **2012**, *94*, 7–10.

(10) Lee, C. K.; Cho, E.; Lee, H. S.; Hwang, C. S.; Han, S. First-Principles Study on Doping and Phase Stability of HfO<sub>2</sub>. *Phys. Rev. B: Condens. Matter Mater. Phys.* **2008**, *78*, 012102.

(11) Zhao, X.; Vanderbilt, D. Phonons and Lattice Dielectric Properties of Zirconia. *Phys. Rev. B: Condens. Matter Mater. Phys.* **2002**, *65*, 075105.

(12) Zhao, X.; Vanderbilt, D. First-Principles Study of Structural, Vibrational, and Lattice Dielectric Properties of Hafnium Oxide. *Phys. Rev. B: Condens. Matter Mater. Phys.* **2002**, *65*, 233106.

(13) Robertson, J. High Dielectric Constant Gate Oxides for Metal Oxide Si Transistors. *Rep. Prog. Phys.* **2006**, *69*, 327–396.

(14) Jinesh, K. B.; Lamy, Y.; Tois, E.; Forti, R.; Kaiser, M.; Bakker, F.; Wondergen, H. J.; Besling, W. F. A.; Roozeboom, F. Cubic Phase Stabilization and Improved Dielectric Properties of Atomic-Layer-Deposited Er<sub>y</sub>Hf<sub>1-y</sub>O<sub>x</sub> Thin Films. *J. Mater. Res.* **2010**, *25*, 1629–1635.

(15) Tomida, K.; Kita, K.; Toriumi, A. Dielectric Constant Enhancement due to Si Incorporation into HfO<sub>2</sub>. *Appl. Phys. Lett.* **2006**, *89*, 142902.

(16) Park, P. K.; Kang, S. W. Enhancement of Dielectric Constant in HfO<sub>2</sub> Thin Films by the Addition of Al<sub>2</sub>O<sub>3</sub>. *Appl. Phys. Lett.* **2006**, *89*, 192905.

(17) Hegde, R. I.; Triyoso, D. H.; Samavedam, E. B.; White, B. E., Jr. Hafnium Zirconate Gate Dielectric for Advanced Gate Stack Applications. *J. Appl. Phys.* **2007**, *101*, 074113.

(18) Hegde, R. I.; Triyoso, D. H. Sub-9 Å Equivalent Oxide Thickness Scaling Using Hafnium Zirconate Dielectric with Tantalum Carbide Gate. *J. Appl. Phys.* **2008**, *104*, 094110.

(19) Triyoso, D. H.; Gregory, R.; Park, M.; Wang, K.; Lee, S. I. Physical and Electrical Properties of Atomic-Layer-Deposited Hf<sub>x</sub>Zr<sub>1-x</sub>O<sub>2</sub> with TEMA<sub>Hf</sub>, TEMA<sub>Zr</sub>, and Ozone. *J. Electrochem. Soc.* **2008**, *155*, H43–H46.

(20) Kuo, Y.; Lin, C. C. A Light Emitting Device Made from Thin Zirconium-Doped Hafnium Oxide High-k Dielectric Film with or without an Embedded Nanocrystal Layer. *Appl. Phys. Lett.* **2013**, *102*, 031117.

(21) Lin, C. C.; Kuo, Y. Memory Functions of Nanocrystalline Cadmium Selenide Embedded ZrHfO High-k Dielectric Stack. *J. Appl. Phys.* **2014**, *115*, 084113.

(22) Lin, C. C.; Kuo, Y.; Zhang, S. Nonvolatile Memory Devices with AlO<sub>x</sub> Embedded Zr-doped HfO<sub>2</sub> High-k Gate Dielectric Stack. *J. Vac. Sci. Technol. B* **2014**, *32*, 03D116.

(23) Wang, C.; Zinkevich, M.; Aldinger, F. The Zirconia-Hafnia System: DTA Measurements and Thermodynamic Calculations. *J. Am. Ceram. Soc.* **2006**, *89*, 3751–3758.

(24) Fischer, D.; Kersch, A. The Effect of Dopants on the Dielectric Constant of HfO<sub>2</sub> and ZrO<sub>2</sub> from First Principles. *Appl. Phys. Lett.* **2008**, *92*, 012908.

(25) Shin, Y.; Min, K. K.; Lee, S. H.; Lim, S. K.; Oh, J. S.; Lee, K. J.; Hong, K.; Cho, B. J. Crystallized HfLaO Embedded Tetragonal ZrO<sub>2</sub> for Dynamic Random Access Memory Capacitor Dielectrics. *Appl. Phys. Lett.* **2011**, *98*, 173505.